Quaternary submarine mass-transport complexes on the southern Continental Slope of Campos Basin characterized by AUV high frequency geophysical data

Anderson Gomes de Almeida, Petrobras/E&P-EXP, Renato Oscar Kowsmann, Petrobras/CENPES, Alberto Garcia Figueiredo Jr/Departamento de Geologia e Geofísica, UFF.

This paper was prepared for presentation during the 14th International Congress of the Brazilian Geophysical Society held in Rio de Janeiro, Brazil, August 3-6, 2015.

Abstract

This study focuses on Submarine Mass Transport Complexes (MTC) in deep water environment on the Continental Slope in the south portion of Campos Basin.

The goal of this work is to show the potential of the autonomous underwater vehicle records in the identification and classification of mass transport deposits.

Multibeam echosounder Simrad EM 2000 (200 kHz) and sub-bottom profiler 216 FSSG Chirp (2 – 10 kHz) data, both from Edgetech, were used in this study.

The main erosional features identified was the scar slump, the amphitheatre scar, the long curved scar (approximately 5 km long), and the extensive (approximately 10 km long) scarps of planar failure.

In the study area the microtopography of the slump deposit is wavy as a response to the internal structures. The undeformed substrate of the MTC is represented by a distinct bottom echo with several parallel continuous internal reflections and are truncated from the headscarp to the scar base. The basal shear surface of the slumps is a very sharp surface echo with no or few diffuse subbottom reflections and with near flat or slightly inclined topography and slightly irregular relief. Usually above the basal shear surface and along the scar base there are acoustically transparent masses possibly comprising blocks and clasts collapsed from the headscarp. The ramp of the basal shear surface marks the limit of substrate removal.

Where the ramp is overlain by mass transport deposits it was classified as frontally emergent. Otherwise in a frontally confined landslide, fold and thrust systems entrenched by frontal ramps occur at the toe domain.

Introduction

This study focuses on Submarine Mass Transport Complexes (MTC) in deep water environment on the Continental Slope in the southern portion of Campos Basin, Brazil. The study area is situated between isobaths -300 m and -1000 m in an area between canyons of the Southeast Canyons Group (Reis, 1994; Viana et al., 1999). The area is cut and bordered on the northwest by Tamoio Canyon (Fig. 1). The upper slope is bordered by an erosional terrace adjacent to northeast trending shelfbeak escarpment (Almeida and Kowsmann, 2011, 2015). According to Kowsmann (2002) in the Campos Basin seabed erosion and mass wasting are associated with the regional physiography, which is largely controlled by the underlying geology and to some extent by geostrophic currents.

Particularly influential are the extensional faults produced by salt flowage due to focussed sediment loading on the upper slope in the past, which often control canyon formation, and the clinoform shape of the thick Miocene prograding wedge that determines the gradients of the middle and lower slope.

The goal of this work is to show the potential use of modern autonomous marine system survey of high frequency marine geophysical data in the identification and classification of mass transport deposits. Acquisition of high frequency geophysical data by Autonomous Underwater Vehicles have revolutionised our ability to image the seafloor, providing higher resolution seafloor mapping data than can be achieved from surface vessels, particularly in deep water (Wynn et al., 2014).

According to Posamentier and Martinsen (2011) the term mass-transport deposit (also known as MTD) encompasses several slope deformational processes, including creep, slide, slump, and debris flow. These processes form a continuum, and are intergradational.

Mass movement of sediments form kilometer-scale features that represent major subaerial and subaqueous geohazards and can comprise significant depositional elements, characterizing marine slope and basin-floor systems (Posamentier and Martinsen, 2011). Mass movement of sediments can significantly affect stability of offshore installations (Prior and Coleman, 1982). As mentioned by Posamentier and Walker (2006), in some deep-water settings, MTC deposits can constitute upwards of 50% of the stratigraphic section.

Data

This study is based in the application of high frequency marine geophysical data. The research vessel Northern Resolution carried out the AUV model C-SURVEYOR II™ with the survey sensors: Multibeam echosounder Simrad EM 2000 (200 kHz); Sub bottom profiler 216 FSSG Chirp (2 – 10 kHz), both from Edgetech. Theses raw data were collected and processed by C&C Technologies.

The survey was carried out with an AUV flying height of 40 m. Multibeam data has 3 meters grid (bin size). The accuracy of bathymetric data is 0.3% of water depth. The SBP has a vertical resolution estimated at 10 cm and penetration range of 150 m from AUV.

The tide corrections were applied to the multibeam data using the forecast generated from oceanic global tide model from NASA (Goddard), which are Topex and Poseidon satellite altimeter based and are referenced to the mean sea level. The depth of AUV was determined by Digiquartz pressure sensor, and the values were added to the multibeam data. The acoustic corrections of water column velocity were applied by using harmonic curves of calculated velocities from CTD profiling performed during survey.

The patch test calibration was used to calculate any misalignment in the mounting of the EM 2000 Multibeam System on the *C-Surveyor II™*. The calibration is performed at sea where angular transducer corrections for roll, pitch, and azimuth (yaw) are calculated empirically. Tracklines run with different parameters and over different features on the seabed are used to calculate these misalignment values. In addition, the patch test can provide information on system latency, repeatability, and accuracy in a true dynamic mode. Repeatability of the system as a whole, as well as for each individual beam (111 totals) or any set of beams, can also be determined.

Method

Damuth (1980) and Lee et al. (2002) presents a review echo-character classification whose criteria were used during this work.

The laterally wedged geometry and the internal acoustic transparency have been recognized as the most conspicuous features of debrites. This transparency reflects the internal homogenization, probably resulting from a disintegration of slope-failed masses by shear deformation and mixing with water during debrisflow formation (Middleton and Hampton, 1973; Nardin et al., 1979).

The scars and scarps, the blocky, lumpy or hyperbolic morphology of the displaced masses with deformed or transparent internal reflectors, and the dominant deformed muds are typical characters of slides and slumps (Mulder and Cochonat, 1996).

The interpretation of Sub bottom profiler (SBP) and Multibeam (MB) data to identify and classify the MTC features and deposits was based on Martínez et al. (2006) classification as frontally confined versus frontally emergent submarine landslides. The kinematic indicators of MTCs based on 3D seismic data (Bull et al., 2008) was used to characterize the MTCs. Although of different scale and data type, the good data quality, resolution of the AUV data allowed an adaptation and application of Bull et al. key geometrical and geological criteria in the study area.

Bull et al. (2008) define a kinematic indicator as a geological structure or feature which records information related to the type and direction of motion at the time of emplacement, and as such they are of great use to our understanding of the initiation, dynamic evolution and cessation of slope failures.

Martínez et al. (2006) propose a classification of frontally confined versus frontally emergent submarine landslides. In the former, the landslide undergoes a restricted downslope translation and does not overrun the undeformed downslope strata. In the latter, much larger downslope translation occurs because the landslide is able to ramp up from its original basal shear surface and translate in an unconfined manner over the seafloor. The differentiation of these two end members is of critical importance as their respective mechanisms of formation, downslope propagation and emplacement are significantly different, and hence need to be taken into consideration when analyzing their respective kinematics.

Results

Several MTC features were identified with multibeam image and SBP profiles. Fig. 1 shows a shaded bathymetric multibeam image and the location of SBP lines selected to describe each MTC feature.

SBP Profile 1 is a scar slump (Fig. 2). The microtopography of the slump deposit is wavy as a response to the internal structures. The undeformed substrate of MTC is represented by distinct bottom echo with several parallel continuous internal reflections that are truncated from the headscarp to the scar base. The very sharp surface echo with no or few diffuse subbottom reflectors and with near flat or slightly inclined topography and with slightly irregular relief characterize the basal shear surface of the slump. Above the basal shear surface and below the scar base there are acoustically transparent masses possibly comprising blocks that fell from the headscarp. The chaotic mass with scattered high amplitude (sharp dots) above the latter are possibly clasts resulting from the disintegration of blocks. An abrupt ramp in the basal shear surface occurs downslope. The ramp marks the limit of substrate removal. This ramp is overlapped by mass transported, and the substrate below the ramp suffered horizontal drag and is deformed into folded strata. This MTC is a frontally emergent submarine landslide. The runout is 2 km, measured downslope from the ramp.

Profile 2 (Fig. 3) passes through the amphitheatre scar (Fig. 1). The head scarp is abrupt and the headwall slope is steep where the substrate outcrops. Below and downslope from the headwall the MTC body is acoustically transparent indicating a disintegrative mass in the translational domain. At the toe domain downslope, the slope decreases and accumulation occurs represented by acoustically chaotic and transparent masses of debris. The MTC suffered frontal compression and deformed into folded strata that produce a wavy topography. A transparent layer continues downslope of the toe domain probably representing a mud flow. The edge of this MTC is outside the survey area. Although the basal ramp is not imaged it is probably situated at the point of slope change. The characteristics mentioned are indicative of a frontally emergent submarine landslide.

Profile 3 (Fig. 4) crosses the long curved and scar (approximately 5 km wide) with at least two stacked events of MTC. The older basal shear surface 1 has irregular, blocky and hyperbolic masses deposited by rock fall translated perpendicular to headwall scarp. Along the basal surface 1, in the translational domain there is no deposition. The basal shear surface 1 ends at the frontal ramp that confines the MTC. That is the toe domain where accumulation occurs, represented by masses of wavy and folded strata. The MTC above the basal shear surface 1 is a frontally confined submarine landslide. In the interval between the basal shear surfaces 1 and 2 occurs a package with distinct bottom echo with several parallel continuous internal reflections. Above the basal shear surface 2 there is no accumulation in the headwall domain. In the translational domain there is depletion and the MTC thickness increases gradually to the toe domain. In this latter domain there is significant accumulation of acoustically chaotic and transparent masses. However the mass transport exceeds the obstacle of underlying MTC and continues beyond the toe domain as a free translating, acoustically transparent layer, as a frontally emergent submarine landslide.

Profile 4 (Fig. 5) is located downslope in relation to Profile 3. The sea bed topography is wavy due to the underlying MTC structures (Fig. 1). Upslope and above the basal shear surface there are localized masses of continuous reflections with well defined edges. These masses are interpreted as outrunner blocks in the translational domain. Internally within the MCT a reflection separates an acoustically transparent layer on the bottom from a chaotic layer on the top. The internal stratification becomes gradually more deformed downslope. At the toe domain there are fold and thrust faults deforming the internal stratification. Although the edge of this MTC is not defined, as it was probably removed by the scar downslope, the structures identified allows us classify it as frontally confined landslide.

Profile 5 (Fig. 6) crosses two extensive (approximately 10 km long) scarps of planar failure with the stepped profile. The undeformed substrate is represented by a distinct bottom echo with several parallel continuous internal reflections that are truncated from the headscarp to the scar base. The very sharp surface echo with no or few diffuse subbottom reflections characterizes the basal shear surface of the MTC. Below the headwall the MTC body has acoustically chaotic reflections indicating debris (blocks and clasts). Downslope, the MTC layer becomes acoustically transparent and subtly wavy. The MTC layer becomes more deformed with pressures ridges and folded strata. The MTC continues downslope over the lower scarp.

Conclusions

The high-frequency marine geophysical data obtained by AUV survey is an excellent tool to characterize Quaternary Mass-Transport Complexes. The bathymetric data from Multibeam echosounder provides high resolution images (grids of 3 m) of the sea bottom where several elemental features that comprise each MTC can be identified. The main erosional features studied was scar slump, the amphitheatre scar, the long curved scar (approximately 5 km wide), extensive (approximately 10 km long) scarps of planar failure. The MTC deposits of these erosional features was described and analyzed in sub-bottom profiler sections that cross the MTCs in the dip direction. The acoustic features of each MTC deposit allowed to infer the deformation structures and facies.

The integration and interpretation of SBP and MB data to identify and classify the MTC features and deposits was based on Martínez et al. (2006) classification in frontally confined versus frontally emergent submarine landslides and the review of kinematic indicator from MTC using 3D seismic data made by Bull et al. (2008). Although of different scales and data type, the good data quality and resolution allowed to adapt and apply the key geometrical and geological criteria of Bull et al. 2008 in the study area. Thus the MTC deposits were divided into headwall, translational and toe domains.

The microtopography of the slump deposit is wavy as a response to the internal structures. The undeformed substrate is represented by distinct bottom echo with several parallel continuous internal reflections which are truncated from the headscarp to the scar base. The very sharp echo with no or few diffuse subbottom reflections and with near flat or slightly inclined topography characterize the basal shear surface of the slumps. Usually above the basal shear surface and below the scar base there are acoustically transparent masses possibly comprising blocks that fell from the headscarp. The chaotic mass with scattered high amplitude above the detachment are possibly clasts resulting from the disintegration of some blocks. The ramp that often occurs at the basal shear surface marks the limit of substrate removal.

A landslide limited by frontal ramps within the toe domain of fold and thrust, with deformed internal stratification was classified as a frontally confined landslide. On the other hand, a mass transport deposit that overstepped the ramp was recognized as a frontal emergent submarine landslide.

Acknowledgments

The authors are thankful to Petrobras for providind the data and to ANP for authorize this to the first author’s master’s thesis at UFF/DOT. The authors gratefully acknowledge the reviewers MSc José Mauricio Caixeta and PhD Pierre Muzzi Magalhaes for their thoughtful comments. Special thanks are due to survey team mates and crew of R/V Northern Resolution.

References

Almeida, A. G., and Kowsmann, R. O., 2011. Caracterização geomorfológica do fundo marinho do talude continental da Bacia de Campos, RJ. 13^{o} Congresso da Associação Brasileira de Estudos do Quaternário, Armação de Búzios, Brasil. São Paulo: Universidade de São Paulo.

Almeida, A. G., and Kowsmann, R. O., 2015. Geomorfologia do Talude Continental e do Platô de São Paulo. In: Geologia e Geomorfologia. Elsevier (in the press).

Bull, S., Cartwright, J., Huuse, M., 2008, A review of kinematic indicators from mass-transport complexes using 3D seismic data. Marine and Petroleum Geology. Vol. **26**, Ed. 7. p. 1132-1151.

Damuth, J. E., 1980, Use of high-frequency (3.5-12 kHz) echograms in the study of near-bottom sedimentation processes in the deep-sea: a review. Marine Geology. Elsevier, n. **38**, 1980. p. 51-75.

Frey-Martínez, J., Cartwright, J., and James, D., 2006, Frontally confined versus frontally emergent submarine landslides: a 3D seismic characterisation. Marine and Petroleum Geology, **23**, 5, 585-604.

Jenner, K. A., Piper, D. J., Campbell, D. C., and Mosher, D. C., 2007, Lithofacies and origin of late Quaternary mass transport deposits in submarine canyons, central Scotian Slope, Canada. Sedimentology, **54**, 1, 19-38.

Kowsmann, R.O., Machado, L.C.R., Viana, A.R., Almeida Jr., W., and Vicalvi, M.A., 2002, Controls on mass-wasting in deep water of the Campos Basin. 34th Offshore Technology Conference; Houston, Texas. Richardson: Society of Petroleum Engineers. p. 1-11.

Lee, S. H., Chough, S. K., Back, G. G., and Kim, Y. B., 2002, Chirp (2–7-kHz) echo characters of the South Korea Plateau, East Sea: styles of mass movement and sediment gravity flow. Marine Geology, 184, **3**, 227-247.

Middleton, G. V., Hampton, M. A., 1973, Sediment gravity flows: mechanics of flow and deposition. In: Middleton, G. V., Bouma, A. H. Turbidity and Deep Water Sedimentation. SEPM, Pacific section, Short Course Lecture Notes, p. 1-38.

Mulder, T., and Cochonat, P., 1996, Classification of offshore mass movements: Journal of Sedimentary Research, v. **66**, p. 43-57.

Nardin, T. R., Hein, F. J., Gorsline, D. S., and Edward, B. D., 1979, A review of mass movement processes and acoustic characteristics, and contrasts in slope and base-of-slope systems versus canyon-fan-basin floor systems. In: Doyle, L. J., Pilkey, O. H. Geology of Continental Slopes. Society of Economic Paleontologists and Mineralogists Special Publication **27**, p. 61-73.

Posamentier, Henry W., Martinsen, Ole J. The character and genesis of submarine mass-transport deposits: insights from outcrop and 3D seismic data. SEPM Special Publication. n. **96**, 2011. p. 7-38.

Prior, D. B.; Coleman, J. M., 1982, Active slides and flows in underconsolidated marine sediments on the slope of the Mississippi Delta. In: Saxov, S.; Nieuwenhuis, J. K. Marine Slides and Other Mass Movements: Proceedings of a North Atlantic Treaty Organization (NATO) Workshop on Marine Slides and Other Mass Movements, Algarve, Portugal, 15-21 Dec. 1980, Ser. 4, **6**, p. 21-49.

Reis, A. T., O Grupo Sudeste de Cânions e sua Relação com a Progradação do Leque São Tomé, RJ. Dissertação de Mestrado. Observatório Nacional. Rio de Janeiro, 1994. p. 124.

Viana, A. R., Almeira, W., and Machado, L. C., 1999, Different styles of canyon infill related to gravity and bottom current processes: examples from the upper slope of SE Brazilian margin. 6th International Congress of the Brazilian Geophysical Society; Rio de Janeiro, Brasil. Sociedade Brasileira de Geofísica. Expanded Abstract 01499.

Wynn, Russell B., et al., 2014, Autonomous Underwater Vehicles (AUVs): Their past, present and future contributions to the advancement of marine geoscience. Marine Geology **352**: 451-468.

Illustrations

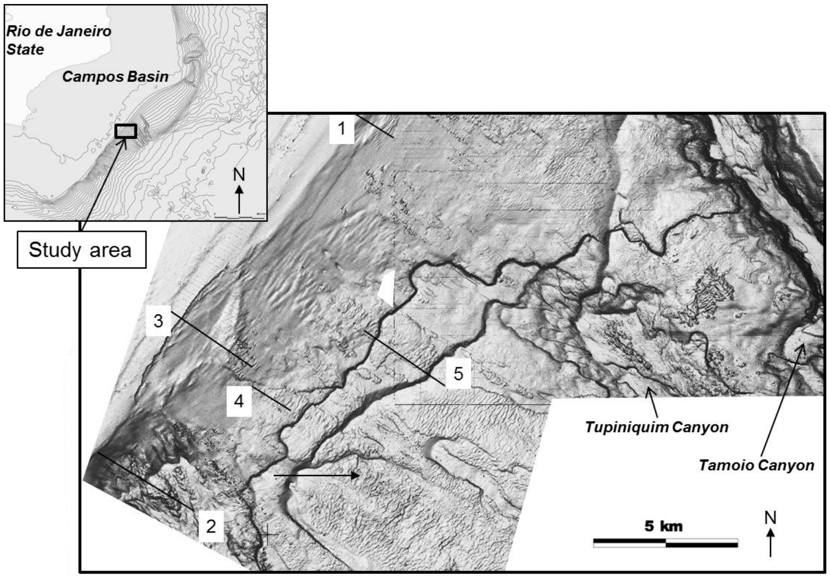

Fig. 1 – Map of study area and multibeam shaded relief image of sea bottom. Sub-bottom profiler lines 1, 2, 3, 4 and 5.

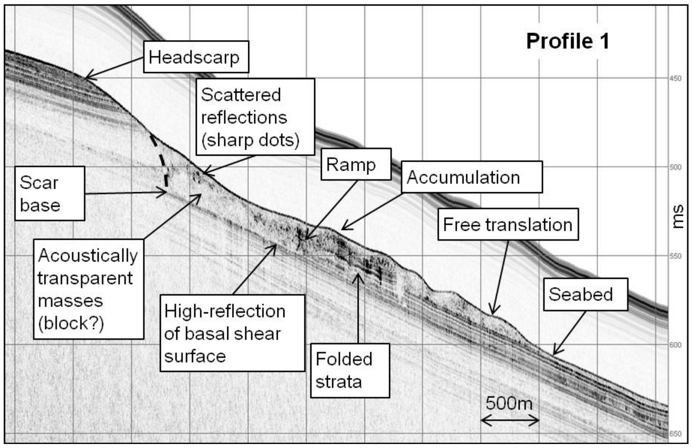

Fig. 2 – SBP Profile 1.

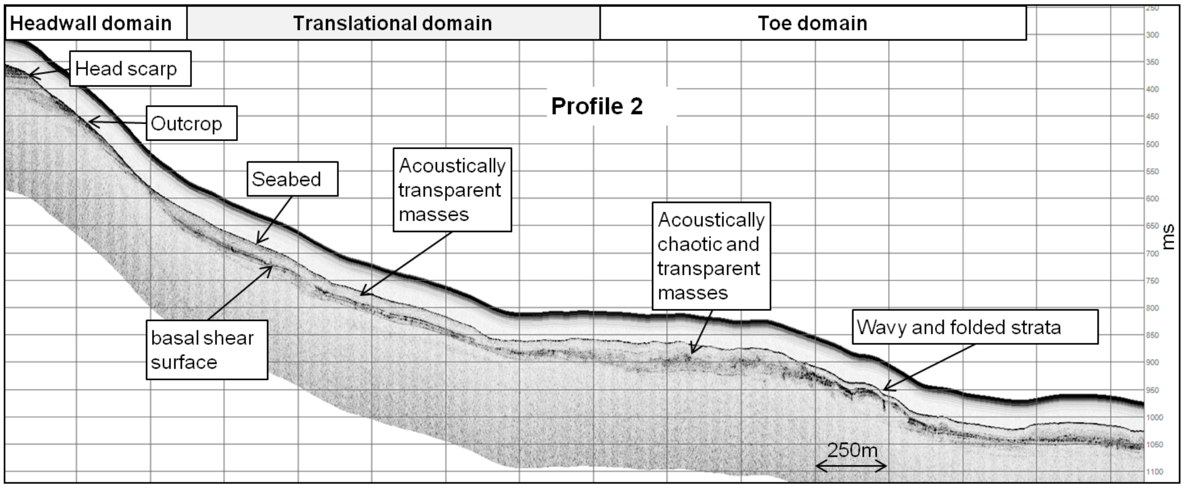

Fig. 3 – SBP Profile 2.

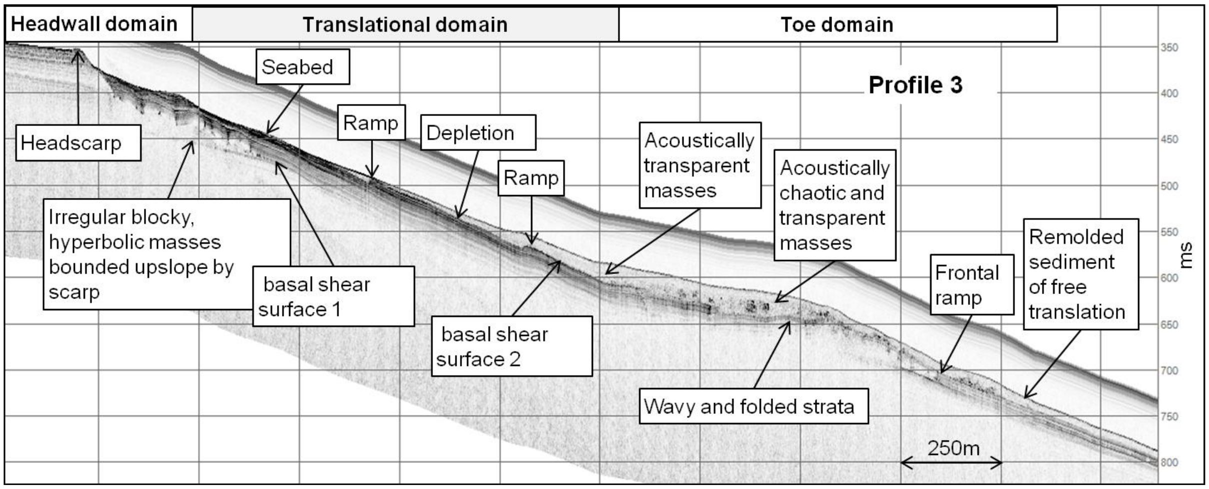

Fig. 4 – SBP Profile 3.

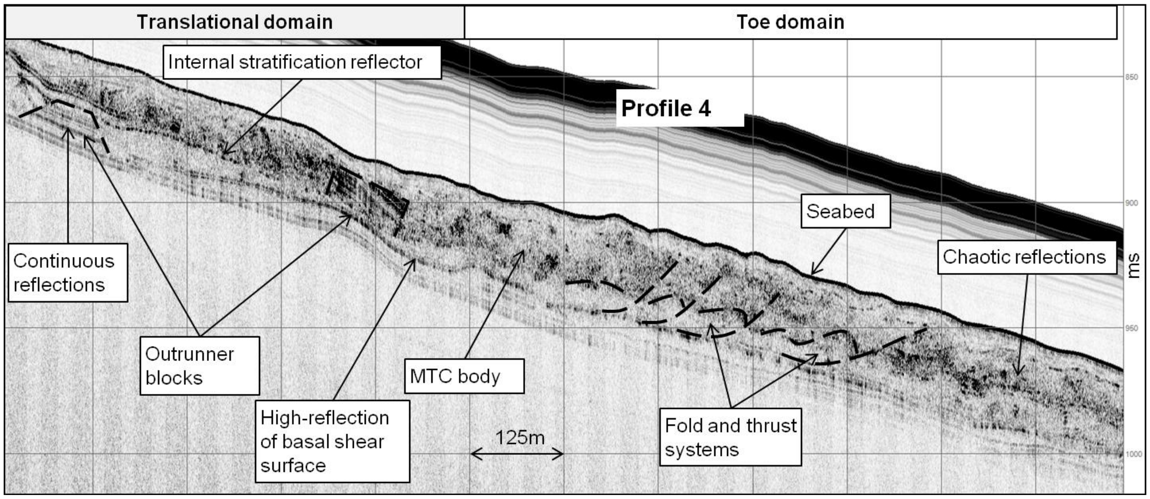

Fig. 5 – SBP Profile 4.

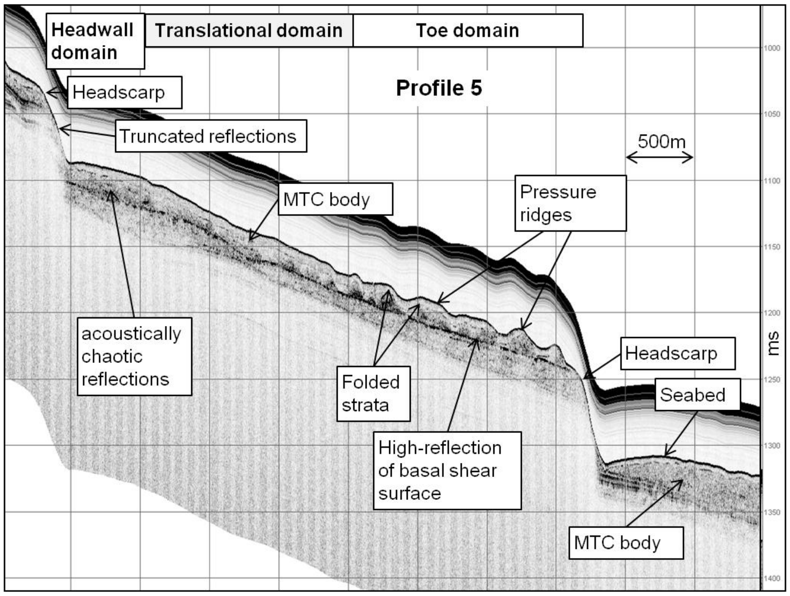

Fig. 6 – SBP Profile 5.